Thickness dependence of the switching voltage in all-oxide ferroelectric thin-film capacitors prepared by pulsed laser deposition

Thickness dependence of the switching voltage in all-oxide ferroelectric thin-film capacitors prepared by pulsed laser deposition

J. F. M. Cillessen,[a] M. W. J. Prins, and R. M. Wolf[b]
Philips Research Laboratories, Prof. Holstlaan 4 5656 AA Eindhoven, The Netherlands

(Received 3 October 1996; accepted for publication 2 December 1996)

Thin-film ferroelectric capacitors consisting of $PbZr_{0.53}Ti_{0.47}O_3$ sandwiched between $La_{0.5}Sr_{0.5}CoO_3$ electrodes have been deposited using pulsed laser deposition. The combination of oxidic perovskite-type materials results in capacitors with a coercive field (E_c) which is comparable with values for bulk ceramics. Textured thin-film capacitors with a columnar microstructure show lower switching voltages than epitaxial films. No thickness dependence of E_c and a good endurance up to 10^{11} cycles have been observed for epitaxial as well as textured capacitors with oxidic electrodes. In contrast, capacitors with a metallic top electrode show an increase of E_c with decreasing thickness of the ferroelectric layer. We show that charge injection can explain the experimentally observed increase of E_c with decreasing ferroelectric layer thickness. An overview is given of the growth conditions needed for $PbZr_{0.53}Ti_{0.47}O_3$ films, because the precise stoichiometry is of the utmost importance for the capacitor quality. © *1997 American Institute of Physics.* [S0021-8979(97)06405-0]

I. INTRODUCTION

$PbTiO_3$ and its lanthanum and/or zirconium substituted derivatives, forming the $[Pb,La](Zr,Ti)O_3$ system, are the most intensively studied ferroelectric materials. Thin films of these materials are interesting for electronic device applications such as nonvolatile memories, infrared and pressure sensors, and integrated optical switches and modulators.[1] In thick ceramic capacitors, the influence of grain size and grain boundaries has been studied in detail.[2] In thin-film capacitors, particularly the influence of the electrode-ferroelectric interface is more pronounced. This is demonstrated by an increased switching voltage (V_{sw}) of ferroelectric thin films compared with extrapolated values of coarse grained ceramics. The integrated application of ferroelectric materials requires films with a submicron thickness to comply with IC voltages of a few volts.[3] This calls for a detailed comprehension of ferroelectric thin films and electrodes. Furthermore, ferroelectric capacitors for memory applications should withstand more than 10^{11} switching cycles.

The beneficial combination of oxidic electrodes and oxidic ferroelectrics was first shown by Pulvari and Srour[4] in 1969. In their work, the use of doped SnO_2 electrodes as compared to silver-paint electrodes considerably reduced the switching voltage and improved the shelf life of thin $Bi_4Ti_3O_{12}$ single-crystal platelets. Several groups reported on the growth and crystallographic characterization of ferroelectric thin films in combination with a variety of oxidic electrode materials.[5–7] Ramesh *et al.*[8] observed low switching voltages in textured $PbZr_xTi_{1-x}O_3$ films on silicon substrates by using a $Bi_4Ti_3O_{12}$ template layer. The fabrication and properties of heteroepitaxial $SrRuO_3$-$PbZr_xTi_{1-x}O_3$-$SrRuO_3$ capacitors on $(100)SrTiO_3$ substrates were reported by Eom *et al.*[9] Important questions remain as to the nature of the electrode-ferroelectric interface. For example, it is unclear if the near-electrode material is ferroelectric and if charge injection is of importance.[10]

In this article, the influence of the electrode material is studied by analyzing the switching voltage as a function of the $PbZr_xTi_{1-x}O_3$ thickness. Results are compared for $PbZr_xTi_{1-x}O_3$ films on oxidic bottom electrodes, with either oxidic or metallic top electrodes. A one-dimensional model is proposed to explain the observed thickness dependence of the switching potential. Second, the influence of the $PbZr_xTi_{1-x}O_3$ microstructure on the switching characteristic of all-oxide capacitors is investigated by comparing single-crystalline capacitors deposited on (100)MgO with textured layers grown on (100)Si. Additionally, the endurance of our capacitors is studied.

II. EXPERIMENTAL ASPECTS

Thin films in a capacitor geometry are deposited using the pulsed laser deposition (PLD) technique. An ArF excimer laser beam (with a wavelength $\lambda = 193$ nm, a pulse width of 15 ns, and a repetition rate of 2 Hz) is focused onto a rotating, sintered target. For the deposition of $La_{0.5}Sr_{0.5}CoO_3$ (the electrode material) a stoichiometric target is used, whereas for $PbZr_{0.53}Ti_{0.47}O_3$ (a chemical composition with a low ferroelectric switching field[11,12]) a PbO-enriched target is used. A detailed description of the stoichiometric growth of $PbZr_{0.53}Ti_{0.47}O_3$ and the reason for PbO target enrichment is presented in the Appendix. The fluence of the incident laser beam on the target is 4 J/cm^2 and the base pressure of the vacuum chamber is in the 10^{-7} mbar range. Films are deposited onto a heated substrate in a 0.2 mbar oxygen partial pressure ambient. After the growth, the sample is cooled to room temperature (10 °C/min) in 1 bar of oxygen. The films are analyzed by secondary-ion-mass spectrometry (SIMS), x-ray diffraction (XRD), and x-ray fluorescence spectroscopy (XRF).

[a]Electronic mail: cillessn@natlab.research.philips.com
[b]Present address: Philips Laboratories, Scarborough Road, Briarcliff Manor, New York.

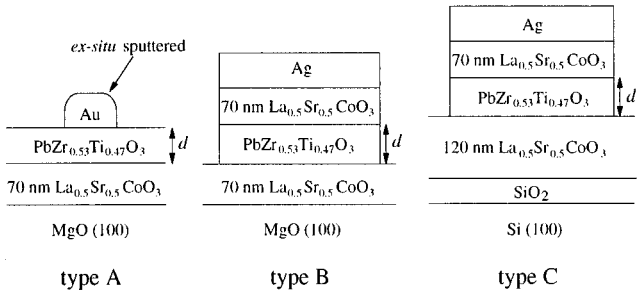

FIG. 1. Three types of samples prepared: all layers were *in situ* grown by PLD except for the sputtered Au electrode. Thickness d is variable.

Three types of samples are prepared as shown in Fig. 1. Samples of type A consist of a MgO(100) substrate with a heteroepitaxial $La_{0.5}Sr_{0.5}CoO_3$ bottom electrode and a heteroepitaxial $PbZr_{0.53}Ti_{0.47}O_3$ film. $La_{0.5}Sr_{0.5}CoO_3$ was chosen since it exhibits a cubic lattice parameter of 0.383 nm[13] and a perovskite-type structure, which both match the ferroelectric material. It has been shown that heteroepitaxial growth of $PbZr_{0.53}Ti_{0.47}O_3$ (0.404 nm) is possible on top of this electrode material.[7,8] Gold top electrodes are *ex situ* Ar sputtered in a scanning electron microscope (SEM)-coating unit (20 kV, 20 mA) onto the heterostructure using a contact mask. The B-type samples are similar to the A types, but the top electrodes consist of *in situ* grown $La_{0.5}Sr_{0.5}CoO_3$. The C-type samples are the same as the B type, but are grown on (100)Si (including native oxide).

$La_{0.5}Sr_{0.5}CoO_3$ films are deposited at a substrate temperature of 650 °C (MgO) and 590 °C (Si). The $La_{0.5}Sr_{0.5}CoO_3$ thickness is 70 nm on MgO and 120 nm on Si. $PbZr_{0.53}Ti_{0.47}O_3$ films with thicknesses d ranging from 50 to 1000 nm are *in situ* deposited on top of the $La_{0.5}Sr_{0.5}CoO_3$ films. The substrate temperature used for $PbZr_{0.53}Ti_{0.47}O_3$ deposition is 587 ± 2 °C (see Appendix). Subsequently, 70 nm $La_{0.5}Sr_{0.5}CoO_3$ top electrodes are *in situ* deposited at 587 °C. In order to ease contacting, top electrodes are silver coated (*ex situ* sputtered). The $La_{0.5}Sr_{0.5}CoO_3$-Ag top layers are structured to form electrode dots of varying sizes using photolithographic processing and Ar-ion etching.

The switching voltage V_{sw} and remnant polarization P_r are determined using a Sawyer–Tower circuit.[14] V_{sw} is also determined by $C-V$ analyses using a probing ac voltage of 0.05 V at 10 kHz and a voltage sweep at a rate of 0.5 V/s. The endurance of a C-type capacitor with a 400 nm $PbZr_{0.53}Ti_{0.47}O_3$ thickness is analyzed by measuring the total as well as the remnant polarization as a function of the number of polarization reversals (N). The applied pulse height during the experiment is ±10 V, the pulse width 100 ns with a delay of 1 μs.

III. RESULTS AND DISCUSSION

We reported the growth and microstructure of $La_{0.5}Sr_{0.5}CoO_3$ films on MgO and Si substrates in an earlier paper.[7] Several other groups also reported on these subjects.[5,15] Despite the 9.8% lattice mismatch between $La_{0.5}Sr_{0.5}CoO_3$ and (100)MgO, heteroepitaxial growth is observed in XRD pole-figures and TEM analyses.[16] XRD patterns of $La_{0.5}Sr_{0.5}CoO_3$ films on MgO(100) showed only sharp (00l) diffraction peaks and a lattice spacing of 0.382 ±0.002 nm was determined. $La_{0.5}Sr_{0.5}CoO_3$ films are smooth, shiny, and black in appearance. The resistivity of epitaxial $La_{0.5}Sr_{0.5}CoO_3$ films is $1.7\pm0.2\times10^{-4}$ Ω cm, a value which is slightly lower than the reported literature value for bulk ceramics.[17] For the growth of $La_{0.5}Sr_{0.5}CoO_3$ films on Si subtrates (including native oxide), we observed a columnar microstructure with an average column diameter of 40 nm. For films deposited at 587 °C, SIMS analysis indicates only a slight interdiffusion between $La_{0.5}Sr_{0.5}CoO_3$ and Si. The resistivity of these $La_{0.5}Sr_{0.5}CoO_3$ films is comparable with our epitaxial films on MgO. Deposition on Si substrates at temperatures above 650 °C results in severe interdiffusion. This is confirmed by the presence of Sr silicates in XRD patterns as well as a strong increase of the $La_{0.5}Sr_{0.5}CoO_3$ resistivity.

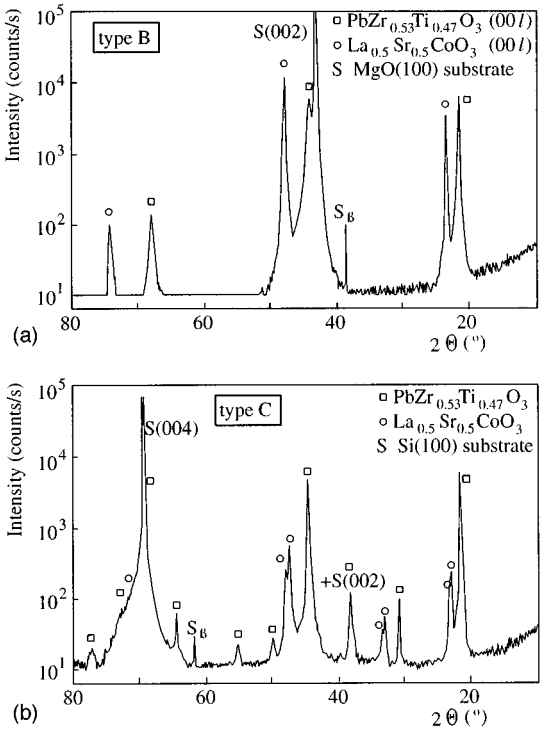

FIG. 2. XRD pattern ($\theta-2\theta$ scan, Cu $K\alpha$ radiation) of: (a) B-type capacitor: $PbZr_{0.53}Ti_{0.47}O_3$ thickness 80 nm, (b) C-type capacitor: $PbZr_{0.53}Ti_{0.47}O_3$ thickness 80 nm.

$PbZr_{0.53}Ti_{0.47}O_3$ films grown on $La_{0.5}Sr_{0.5}CoO_3$ electrodes on MgO (capacitor types A and B) are heteroepitaxial as indicated by the XRD pattern in Fig. 2(a). A detailed growth study of epitaxial $PbTiO_3$ films on a variety of materials with different lattice parameters was published earlier.[18] For the C-type capacitors, a columnar growth with a preferential (00l) orientation is observed for both $La_{0.5}Sr_{0.5}CoO_3$ and $PbZr_{0.53}Ti_{0.47}O_3$ films. This can be described by grain-to-grain epitaxy: each $PbZr_{0.53}Ti_{0.47}O_3$ grain shows an epitaxial relation with a grain from the bottom electrode and the top electrode.[7] The XRD pattern of such capacitors [Fig. 2(b)] indicates the presence of two distinct $La_{0.5}Sr_{0.5}CoO_3$ lattice parameters of 0.381 and 0.384 nm, respectively. A

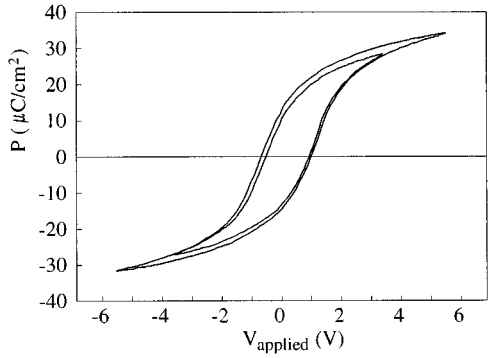

FIG. 3. Hysteresis loops measured with a Sawyer–Tower circuit. The outer loop (±5.5 V amplitude) shows nearly the same hysteresis behavior as the inner loop (±3.5 V), which is due to the saturation of ferroelectric polarization. The $PbZr_{0.53}Ti_{0.47}O_3$ thickness is ≈600 nm.

shift of the bottom electrode lattice parameters is most probably caused by built-in strain.

Typical hysteresis loops, measured for two different voltage sweeps, for C-type samples are shown in Fig. 3. P_r values are 20 ± 5 $\mu C/cm^2$. For all samples the switching potential (V_{sw}) as a function of the $PbZr_{0.53}Ti_{0.47}O_3$ thickness is shown in Fig. 4. The differential coercive fields $\Delta V_{sw}/\Delta d$, calculated from the slopes for different types of capacitors are 21 ± 3 (type A), 23 ± 4 (type B), and 12 ± 4 kV/cm (type C). It is striking that the slopes for the A- and B-type samples are similar. This shows that the differential coercive field is independent on the type of top electrode and directly refers to the intrinsic properties of the $PbZr_{0.53}Ti_{0.47}O_3$ film. The C-type samples show a significantly lower coercive field, approaching the value for bulk material.[12] The microstructural difference between the B- and C-type samples indicates that a textured microstructure facilitates ferroelectric switching. From bulk ceramics it is well known that the switching field is related to the microstructure. In our single crystalline samples (B type), ferroelectric domain wall motion is obviously hindered by the lack of grain boundaries, which results in an increase of V_{sw}. Studies on $[Pb,La](Zr,Ti)O_3$ capacitors by Ramesh *et al.*[8] also indicate a lowering of V_{sw} for a textured microstructure.

From Fig. 4, it appears that the extrapolated switching potential to zero film thickness is different for *ex situ* sputtered gold (A type) and *in situ* grown $La_{0.5}Sr_{0.5}CoO_3$ top electrodes (B and C type). For the A-type samples, the intercept is 1 V, whereas for the B- and C-type samples the intercepts are close to zero. As a consequence, $E_c(=V_{sw}/d)$ for the A-type samples is increasing for films below 500 nm. These results suggest that the offset voltage as observed for the A-type samples, is related to an interface effect rather than to a bulk effect. A model to explain the observed thickness dependence of the switching potential is described in Sec. IV.

For applications, the endurance of ferroelectric capacitors is important. The results of Fig. 5 show that C-type samples do not degrade within 10^{11} switching cycles. The switching polarization tends to increase slightly with the number of switching cycles. This is attributed to a poling of

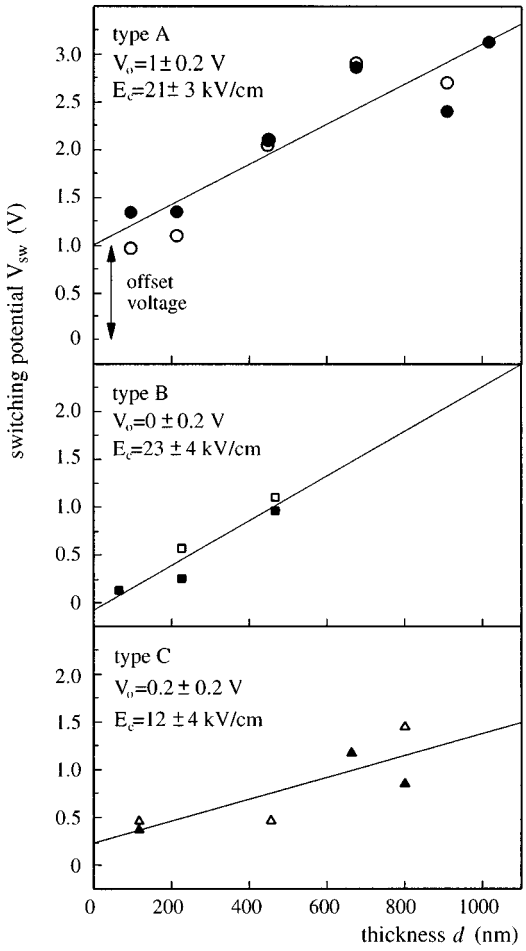

FIG. 4. Switching potential (V_{sw}) vs $PbZr_{0.53}Ti_{0.47}O_3$ film thickness for A-, B-, and C-type capacitors: filled symbols are taken from $C-V$ measurements, open symbols are taken from hysteresis loops. Note the voltage offset for A-type samples. E_c originates from the calculated slopes.

the capacitor, i.e., a field induced effect which causes an increasing part of the capacitor to switch. Since the ionic displacement in pseudocubic $PbZr_{0.53}Ti_{0.47}O_3$ is small, the energy involved to reorient domains is relatively small. Since

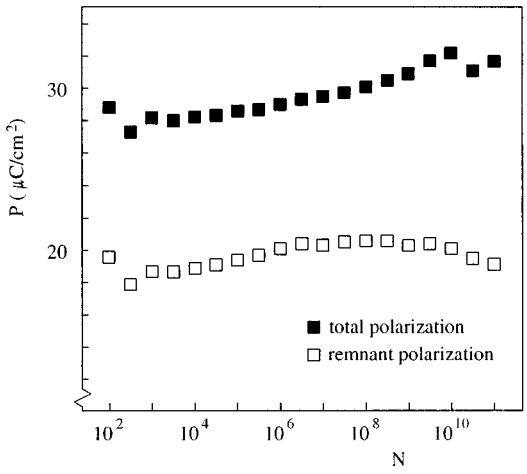

FIG. 5. Endurance of a C-type sample ($PbZr_{0.53}Ti_{0.47}O_3$ thickness 400 nm): the total and remnant polarization are measured vs the number of polarization reversals (N).

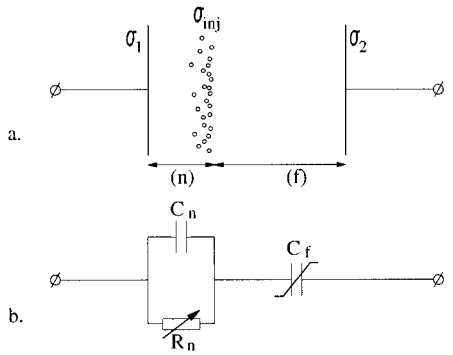

FIG. 6. (a) Model and (b) equivalent circuit to describe charge injection into a near-electrode region of a ferroelectric thin-film capacitor. *n* refers to the near-electrode region, *f* is the ferroelectric material, and R_n is a nonlinear resistor, which allows the flowing of an injection current.

most of the $PbZr_xTi_{1-x}O_3$ compositions are efficient piezoelectric materials, ferroelectric capacitors must be able to withstand mechanical stresses induced by electrical fields. We assume that the good endurance of our capacitors is related to the chemical stability (low interdiffusion) as well as the mechanical strength of oxidic interfaces.

In addition to the experiments described, heteroepitaxial capacitors consisting of $PbZr_{0.53}Ti_{0.47}O_3$ sandwiched between $SrRuO_3$ electrodes on $SrTiO_3(100)$ substrates have also been investigated. The lattice match of $SrRuO_3$ ($a=0.394$ nm) with the ferroelectric ($a=0.404$ nm) as well as the substrate ($a=0.390$ nm) is better than for the abovementioned samples. However, we did not observe an improved capacitor quality for $SrRuO_3$ electrodes as compared with $La_{0.5}Sr_{0.5}CoO_3$ in terms of E_c or endurance.

IV. INJECTION MODEL

Our measurements as well as the experimental results of other publications[19,20] demonstrate that in ferroelectric thin-film capacitors with at least one non-oxidic electrode, E_c increases with decreasing $PbZr_xTi_{1-x}O_3$ thickness. In other words, the switching voltage of thin-film capacitors is larger than expected from extrapolated bulk ferroelectric properties. Although it is clear that the presence of the electrode/ferroelectric interfaces is decisive, the nature of the interfacial disorder and the physical properties of the near-electrode material are still under debate. In this section, we describe a one-dimensional model of a ferroelectric thin-film capacitor, we indicate why charge injection into the near-electrode regions can be of importance, and explain the consequence of charge injection for the switching potential.

In the thin-film capacitor, we define a near-electrode region with an electric polarizability which is different from the polarizability of the ferroelectric material.[21] This is schematically shown in Fig. 6(a), for the case of a single nonideal near-electrode region.[22] Region ''*f*'' refers to the ferroelectric part of the capacitor, while region ''*n*'' corresponds to the nonideal near-electrode layer. σ_1 is the charge density present on electrode (1), σ_2 refers to the charge density on electrode (2). It follows from Gauss' law that $\sigma_1=D_n\equiv\epsilon_0E_n+P_n$, where D_n equals the dielectric displacement, E_n is the electric field, and P_n is the electric polarization, all parameters in the *n* region. In order to estimate the electric field in the *n* layer, let us assume that the *n* region shows a dielectric behaviour. In that case $P_n=(\epsilon_r-1)E_n$, where ϵ_r is the relative permittivity, and the electric field in the *n* region is given by: $E_n=\sigma_1/\epsilon_0\epsilon_r$. When ϵ_r equals 100 or less, and for a charge density of the order of 10 μC/cm^2 (see Sec. III), we find an electric field in the *n* region of 1 MV/cm or larger, such that charge injection can realistically take place.

A simple equivalent electrical circuit to describe charge injection is shown in Fig. 6(b). The charge density injected across the *n* region, into trap states for example, is described by σ_{inj} [Fig. 6(a)]. Charge exchange through the *n* layer across capacitor C_n is allowed by the nonlinear resistor R_n. Although the *n* and *f* layers are of a different nature, it is clear in that both layers the charge displacement involves the dissipation of energy and gives rise to a hysteresis behavior. The hysteresis of the *f* layer is due to ferroelectricity, i.e., an ionic displacement within each unit cell, whereas the hysteresis behaviour of the *n* layer is caused by charge exchange between the electrode and near-electrode trap states. In the *n* layer, the ''coercive field'' is determined by the threshold field for charge transport across that layer, i.e., the field needed to inject carriers or to liberate previously injected trapped charge. The total switching potential V_{sw} of the serial arrangement of the *n* and *f* layer is the sum of the individual switching potentials:[23]

$$V_{sw}=V_{sw,n}+V_{sw,f}=d_nE_{th,n}+d_fE_{c,f}=d_n(E_{th,n}-E_{c,f})+d_{tot}E_{c,f}, \qquad (1)$$

where $d_{tot}=d_n+d_f$ is the total film thickness, d_n and d_f represent the thickness of layer *n* and *f* respectively, $E_{th,n}$ is the threshold field in layer *n* and $E_{c,f}$ is the coercive field in layer *f*. As long as the threshold electric field $E_{th,n}$ is not reached, no charge is injected into the *n* layer; then $V_{sw,n}=0$ and the switching potential of the total capacitor equals to the coercive potential of the ferroelectric layer. In the case that injection into the *n* layer takes place, the switching potential of the total capacitor is *larger* than the coercive potential of the single ferroelectric layer. Equation (1) is in good agreement with the experimental results of Fig. 4, showing a linear dependence of the switching potential on the total film thickness, and a nonzero value of the switching potential towards zero film thickness. The increase of the observed switching voltage as shown in Fig. 4 cannot be explained by assuming only a series capacitor as an electrical equivalent for the *n* layer (and thus neglecting charge injection). In such a case the switching potential is not changed although a higher voltage is required for charge displacement. This is experimentally demonstrated in Fig. 7.

In Fig. 4 the differential coercive field $\Delta V_{sw}/\Delta d_{tot}$ equals the true coercive field of the ferroelectric layer $E_{c,f}$. The equivalence of the $PbZr_{0.53}Ti_{0.47}O_3$ films in the A-type as well as the B-type samples is confirmed by a similar slope for these capacitors. This has already been discussed in Sec. III, where 'the bulk of the $PbZr_{0.53}Ti_{0.47}O_3$ film' refers to *f* region from this model. From the experimentally determined

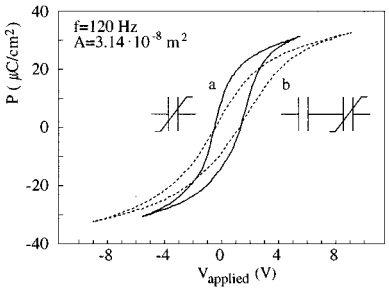

FIG. 7. Hysteresis loop of (a) (solid line) a C-type ferroelectric capacitor and (b) (dashed line) the same sample measured with a 4.4 nF series capacitor. Note that the coercive voltage does not change when the additional capacitor is introduced in the circuit. Only a series capacitor cannot explain the increase of V_{sw}.

Y-axis intercept in Fig. 4 (between 0 and 1 V switching potential), and a threshold for charge transport ($E_{th,n}$) of the order of 1 MV/cm ($E_{c,f}$ is nearly two orders of magnitude smaller), we estimate the thickness of the *n* layer to be 10 nm or less in our samples.

From our model, we expect the dependence of the switching field (V_{sw}/d_{tot}) on the total film thickness to be reduced if charge injection is absent. Charge injection is avoided by using interfaces which do not affect the polarizability of the near-electrode material. In our experiments, we observe superior characteristics for $PbZr_{0.53}Ti_{0.47}O_3$ capacitors sandwiched between oxidic electrodes (type B and C), when compared to the non-ideal behavior of capacitors with an *ex situ* sputtered Au top electrode (type A). The Au electrodes can affect the polarizability of the near-electrode $PbZr_{0.53}Ti_{0.47}O_3$ material by the formation of point defects or a space-charge layer, or by local compositional variations. The latter might be introduced by preferential sputtering of oxygen[24] or lead from the topmost $PbZr_{0.53}Ti_{0.47}O_3$ layer during deposition of the metallic electrode. The use of *in situ* grown oxidic electrodes prevents such problems.

V. CONCLUSIONS

The switching of capacitors with a metallic (*ex situ* sputtered Au) electrode requires higher voltages than capacitors with *in situ* grown oxidic electrodes. The higher switching voltage can be explained by charge injection into a nanometer-thick layer near the electrode. Second, when using only oxidic electrodes, the switching voltage is lower for textured ferroelectric layers (grown on Si) than for heteroepitaxial layers (on MgO). Finally, all-oxide ferroelectric capacitors can withstand more than 10^{11} switching cycles. Summarizing, without the need for an epitaxial relation with the substrate, thin-film $PbZr_{0.53}Ti_{0.47}O_3$ capacitors combined with oxidic electrodes are interesting candidates for low-voltage switching applications.

ACKNOWLEDGMENTS

The authors thank P. K. Larsen and G. L. M. Kampschoër for ferroelectric analyses. They also acknowledge P. C. Zalm and R. C. M. de Kruif for SIMS analyses, M. Kraan and W. C. Keur for target preparations, J. B. Giesbers for microstructuring, and M. H. J. Bekkers for XRF analyses. Furthermore, they thank D. M. de Leeuw, P. W. M. Blom, L. F. Feiner, and M. S. de Keijser for stimulating discussions.

APPENDIX: THE GROWTH OF $PbZr_xTi_{1-x}O_3$ FILMS

The preparation of ferroelectric capacitors requires a detailed study on the stoichiometry of the ferroelectric component. In this Appendix we describe the conditions needed for the growth of high quality $PbZr_xTi_{1-x}O_3$ films and discuss the reactions involved in the formation of this material. From the bulk chemistry it is known that single-phase $PbTiO_3$ can be prepared at temperatures as low as 160 °C by precipitation from aqueous solutions.[25] For vacuum deposited crystalline thin films, temperatures above 350 °C have been reported.[26] At higher substrate temperatures, the crystalline quality and density of the film significantly increases due to the enhanced surface mobility of the species deposited. Especially for epitaxial films with a low orientational spread (narrow XRD rocking curve), a substrate temperature around 600 °C or higher is preferred. A second reason for the use of high temperatures, is the possible formation of the nonferroelectric pyrochlore-type phase $Pb_2Ti_2O_7$ below 400 °C. It is difficult to convert this material into the perovskite-type phase by post-deposition annealing due to its high chemical stability. The formation of pyrochlore-type phases will not be discussed in this article. It is a generally known problem for this materials system and is well documented in the literature.[27]

During the deposition process, species approaching the substrate may either adsorb to the surface, form $PbZr_xTi_{1-x}O_3$, and adhere to the substrate, or desorb from the surface before formation of the preferred compound can take place. Despite the presence of a variety of species in the plasma plume, the major components involved in the formation of $PbZr_xTi_{1-x}O_3$ can be sketched as shown below:

$$\mathrm{Pb}_g \leftarrow (2) \rightarrow \mathrm{Pb}_{\mathrm{ads}}$$

$$\mathrm{Pb}_g + \tfrac{1}{2}\mathrm{O}_2 \leftarrow (3) \rightarrow \mathbf{PbO}_g \leftarrow (4) \rightarrow \mathrm{PbO}_{\mathrm{ads}}$$

$$\mathrm{Ti}_g + \mathrm{O}_2 \leftarrow (5) \rightarrow \mathbf{TiO}_{2\ g} \leftarrow (6) \rightarrow \mathrm{TiO}_{2\ \mathrm{ads}}$$

$$\mathrm{Zr}_g + \mathrm{O}_2 \leftarrow (7) \rightarrow \mathbf{ZrO}_{2\ g} \leftarrow (8) \rightarrow \mathrm{ZrO}_{2\ \mathrm{ads}}$$

$$\mathrm{PbO}_{\mathrm{ads}} + (1-x)\mathrm{TiO}_{2\ \mathrm{ads}} + x\,\mathrm{ZrO}_{2\ \mathrm{ads}} \leftarrow (9) \rightarrow \mathrm{PbZr}_x\mathrm{Ti}_{1-x}\mathrm{O}_{3\ \mathrm{ads}}.$$

According to these equations four species are involved in the formation of $PbZr_xTi_{1-x}O_3$, namely, TiO_2, ZrO_2, Pb, and PbO. For the following description, a substrate temperature of 600 °C is assumed. The relevant properties of species at the used growth temperature are listed in Table I. Ablation from oxidic targets will produce the oxidized species as represented in bold in Eqs. (2)–(9). Due to the large heat of formation a reduction of TiO_2 or ZrO_2 [Eqs. (5) and (7)] in the plasma is not expected for oxygen partial pressures higher than 10^{-6} mbar.[28] Furthermore, the affinity of TiO_2 and ZrO_2 towards oxidic surfaces and the low vapor pressure of both species imply a sticking probability of one [Eqs. (6) and (8)]. As a consequence TiO_2 and ZrO_2 will be present at the substrate surface in the same ratio as in the target.[29] This

TABLE I. Properties of the species of importance for the formation (Ref. 32) of $PbZr_xTi_{1-x}O_3$.

Material	$\Delta G^0_{60\,°C}$ (kJ/mol)	Vapor pressure at 600 °C (see Ref. 33) (mbar)
Pb		3.5×10^{-4}
PbO	−292.7	1.5×10^{-4}
TiO_2	−1010.0	$<10^{-8}$
ZrO_2	−1163.7	$<10^{-8}$
$PbTiO_3$	−1319.8	

is different for PbO, which exhibits a much smaller heat of formation at the temperature used. Therefore a reduction towards metallic lead is likely to take place. The tendency of Pb to evaporate is high, because of the high vapor pressure. Moreover, the sticking probability for metallic Pb on oxidic surfaces is expected to be low (Eq. (2)). According to Eq. (3), the reduction of PbO can be suppressed by applying a high oxygen pressure during deposition. An additional difficulty which might cause a lead deficiency in the film is the high vapor pressure of PbO. In summary, this means that a competition takes place between the formation of $PbZr_xTi_{1-x}O_3$ (which is thermodynamically likely, due to the large $\Delta G^0_{600\,°C}$) and the desorption of PbO [Eq. (4)].

Here, we analyze the precise cation stoichiometry [Pb]/[Ti] for films of $PbTiO_3$, which is the basic compound of the $PbZr_xTi_{1-x}O_3$ materials system. The growth of $PbTiO_3$ films at elevated temperature is controlled by three important parameters: the target composition, the oxygen partial pressure, and the substrate temperature during deposition. Experiments are carried out with a fixed target composition using various deposition temperatures and oxygen partial pressures. Targets consist of 70 wt % $PbTiO_3$ and 30 wt % PbO[30] which corresponds with a molar ratio [Pb]/[Ti]=1.58. First, the cation stoichiometry as a function of the substrate temperature is investigated. The [Pb]/[Ti] ratio recovered in the film for temperatures below 400 °C is similar to the target composition [Fig. 8(a)]. This confirms that stoichiometry is retained during the transport of material from the target into the gas phase.[31] When the substrate temperature is increased, the elemental composition of the film starts to deviate from the target. The reduced [Pb]/[Ti] ratio in the film is therefore attributed to a reduced sticking probability for lead at high substrate temperatures. Second, the influence of the oxygen partial pressure during deposition on the cation stoichiometry in the film is analyzed. As shown in Fig. 8(b), an oxygen partial pressure higher than 3×10^{-2} mbar is necessary to shift the equilibrium of Eq. (3) to the right-hand side. Below the critical pressure of 3×10^{-2} mbar a multiphase film with an overall Pb deficiency is formed consisting of $PbZr_xTi_{1-x}O_3$, anatase-TiO_2 and ZrO_2. This is confirmed by XRD patterns and XRF elemental analyses. Similar critical oxygen pressures have been obtained by Tabata *et al.*[26]

As a conclusion, the observations have serious implications for the growth of epitaxial $PbZr_xTi_{1-x}O_3$ films: once a certain target composition (viz. the excess PbO) is chosen, the deposition parameters regarding the oxygen partial pressure as well as the substrate temperature are fixed.

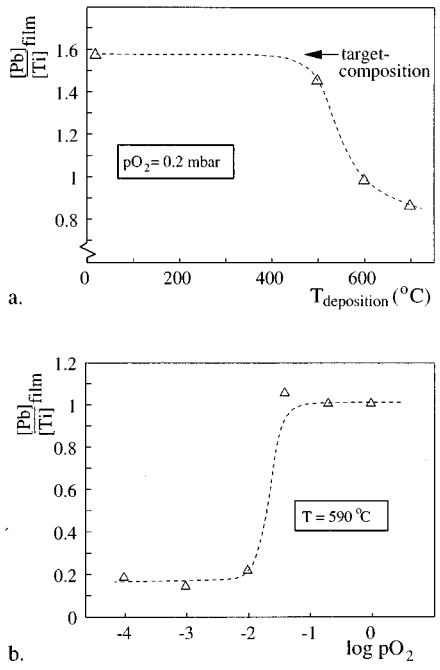

FIG. 8. Cation stoichiometry of $PbTiO_3$ films, analyzed by XRF: (a) [Pb]/[Ti] ratio as a function of the substrate temperature using an oxygen partial pressure of 0.2 mbar, (b) [Pb]/[Ti] ratio as a function of the oxygen partial pressure at 587 °C. The lines are guides to the eye.

[1] G. H. Haertling, J. Vac. Sci. Technol. A **9**, 414 (1991).
[2] R. Waser and M. Klee, Integr. Ferroelectr. **2**, 23 (1992).
[3] R. Moazzami, Semicond. Sci. Technol. **10**, 375 (1995).
[4] C. F. Pulvari and J. R. Srour, IEEE Trans. Electron Devices **16**, 532 (1969).
[5] T. Nakamura, Y. Nakao, A. Kamisawa, and H. Takasu, Appl. Phys. Lett. **65**, 1522 (1994).
[6] S. D. Bernstein, T. Y. Wong, Y. Kisler, and R. W. Tustison, J. Mater. Res. **8**, 12 (1993).
[7] J. F. M. Cillessen, R. M. Wolf, and A. E. M. De Veirman, Appl. Surf. Sci. **69**, 212 (1993).
[8] R. Ramesh, H. Gilchrist, T. Sands, V. G. Keramidas, R. Haakenaasen, and D. K. Fork, Appl. Phys. Lett. **63**, 3592 (1993).
[9] C. B. Eom, R. B. Van Dover, J. M. Phillips, D. J. Werder, J. H. Marshall, C. H. Chen, R. J. Cava, R. M. Fleming, and D. K. Fork, Appl. Phys. Lett. **63**, 2570 (1993).
[10] Charge injection in ferroelectric thin films has already clearly been identified in field-effect transistors with a ferroeletric gate insulator, see, for example, S.-Y. Wu, IEEE Trans. Electron Devices **21**, 499 (1974), or C. H. Seager, D. McIntyre, B. A. Tuttle, and J. Evans, Integr. Ferroelectr. **6**, 47 (1995).
[11] Generally, bulk ceramic properties of ferroelectrics strongly depend on the preparation route (grainsize, density). This is reflected by scattering of physical parameters of $PbZr_{0.53}Ti_{0.47}O_3$, the remnant polarization $P_r = 40\ \mu C/cm^2$, the coercive field $E_c = 8-13$ kV/cm and the relative permittivity ϵ_r ranges between 800 and 1000.
[12] Landolt Börnstein, 16a, Ferro-electrics and related substances, subvolume on oxides, pp. 119–125 (Ikeda).
[13] Rectified value for JCPDS $La_{0.5}Sr_{0.5}CoO_3$, filenr. 36–1394.
[14] C. B. Sawyer and C. H. Tower, Phys. Rev. **35**, 269 (1930).
[15] J. T. Cheung, P. E. D. Morgan, D. H. Lowndes, X-Y. Zheng, and J. Breen, Appl. Phys. Lett. **62**, 2045 (1993).
[16] Selected area electron diffraction (SAED) analyses on cross-section TEM samples in our previous studies showed a doubling of the lattice parameter in $La_{0.5}Sr_{0.5}CoO_3$ films (Ref. 7). In our films, this is definitely not the result of the specimen preparation for XTEM as suggested by Ghonge *et al.* in S. G. Ghonge, E. Goo, R. Ramesh, T. Sands, and V. G. Keramidas, Appl. Phys. Lett. **63**, 1628 (1993). Doubling of the lattice parameter is a phenomenon which is often found in perovskite-type materials. It can be observed using neutron or electron diffraction analyses. In contrast to

XRD, these techniques are capable of detecting the lattice-parameter doubling, due to a higher sensitivity for the oxygen positions in the unit cell. The unit cell doubling, however, does not change the in-plane lattice relation and therefore epitaxy is not affected. Literature on this subject. Landolt Börnstein III, 7e: $PbMg_{0.33}Nb_{0.67}O_3$, p. 521; H. B. Krause and D. L. Gibbon, Z. Krist, **134**, 44 (1971); D. M. de Leeuw, C. A. H. A. Mutsaers, R. A. Steeman, E. Frikkee, and H. W. Zandbergen, Physica C **158**, 391 (1989).
[17] G. H. Jonker and J. H. van Santen, Physica (Amsterdam) **19**, 120 (1953).
[18] A. E. M. De Veirman, J. Timmers, F. J. G. Hakkens, J. F. M. Cillessen, and R. M. Wolf, Philips J. Res. **47**, 185 (1993).
[19] P. K. Larsen, G. J. M. Dormans, D. J. Taylor, and P. J. van Veldhoven, J. Appl. Phys. **76**, 2405 (1994).
[20] Cz. Pawlaczyk, A. K. Tagantsev, K. Brooks, I. M. Reaney, R. Khssurska, and N. Setter, Integr. Ferroelectr. **8**, 293 (1995).
[21] The presence of a layer with low polarizability is demonstrated by small-signal high-frequency capacitance measurements of ferroelectric thin-film capacitors: J. J. Lee, C. L. Thio, and S. B. Desu, J. Appl. Phys. **78**, 5073 (1995).
[22] The addition of a nonideal near-electrode layer (2) does not modify the conclusions of this section.
[23] In practice the switching potential of a thin film is not a constant, but weakly depends on the maximum field experienced in a given hysteresis loop. For clarity this effect is neglected in the present analysis.
[24] R. C. Neville and B. Hoeneisen, J. Appl. Phys. **46**, 350 (1975).
[25] M. M. Lencka, and R. E. Riman, J. Am. Ceram. Soc. **76**, 2649 (1993).
[26] H. Tabata, T. Kawai, S. Kawai, O. Murata, J. Fujioka, and S. Minakata, Appl. Phys. Lett. **59**, 2354 (1991).
[27] J. Lee, A. Safari, and R. L. Pfeffer, Appl. Phys. Lett. **61**, 1643 (1992); H. Adachi and K. Wasa, Mater. Res. Soc. Symp. Proc. **200**, 103 (1990).
[28] A partial oxygen pressure of 10^{-6} mbar roughly corresponds to a monolayer occupation per second, which will do for the deposition rates of 0.1–0.3 nm/s used here.
[29] Analyses of the Zr and Ti content of our films were carried out by Rutherford backscattering spectroscopy (RBS) and XRF. Zr/Ti ratios were similar to the target composition for all ambients.
[30] This specific target composition is derived from preliminary experiments which roughly indicated the excess PbO corresponding with a substrate temperature necessary for epitaxial growth.
[31] The sticking probability of ablated species on room temperature substrates is unity.
[32] I. Barin and O. Knacke, *Thermodynamical Properties of Inorganic Substances* (Springer, Berlin, 1973). To our knowledge the thermodynamic data for PbZr, TiO_3 are not available yet, but we assume that those values are comparable with those for $PbTiO_3$.
[33] Inficon Leybold-Heraeus Co.: 'Material Evaporation Guide' & EPI. ''Vapor Pressure charts.''